LJMU Research Online

Troelsen, P, Wilkinson, D, Seddighi, M, Allanson, D and Falkingham, PL

 Functional morphology and hydrodynamics of plesiosaur necks: Does size matter?

http://researchonline.ljmu.ac.uk/id/eprint/10242/

Article

For more information please contact researchonline@ljmu.ac.uk

http://researchonline.ljmu.ac.uk/

Functional morphology and hydrodynamics of plesiosaur necks: Does size matter?

PERNILLE V. TROELSEN,*,[1] DAVID M. WILKINSON,[2] MEHDI SEDDIGHI,[3] AND

DAVID R. ALLANSON,[3] and PETER L. FALKINGHAM[1]

[1]School of Natural Sciences and Psychology, Liverpool John Moores University, 3 Byrom

Street, Liverpool, Merseyside, L3 3AF, United Kingdom, troelsen_4@hotmail.com and

p.l.falkingham@ljmu.ac.uk;

[2]School of Life Sciences, University of Lincoln, Brayford Pool, Lincoln, LN6 7TS, United

Kingdom, dwilkinson@lincoln.ac.uk;

[3]Department of Maritime and Mechanical Engineering, Liverpool John Moores University, 3

Byrom Street, Liverpool, Merseyside, L3 3AF, United Kingdom, m.seddighi@ljmu.ac.uk

and d.r.allanson@ljmu.ac.uk

---

* Corresponding author.

ABSTRACT—Plesiosaurs are an enigmatic, diverse extinct group of Mesozoic marine reptiles well-known for their unique body plan with two pairs of flippers and usually an elongated neck. The long neck evolved several times within the clade, yet the evolutionary advantages are not well understood. Previous studies have mainly focused on swimming speeds or flipper locomotion. We evaluated the hydrodynamics of neck length and thickness in plesiosaurs using computational fluid dynamics (CFD) simulations based on the Reynolds-Averaged Navier-Stokes (RANS) approach. Simulations were performed of flow patterns forming around five distinctive plesiosaur models, three of different neck lengths (neck/body ratios of 0.2, 0.41, and 0.63) and two of different neck thicknesses (100% and 343% increase compared to cervical vertebrae width). By simulating water flow past the three-dimensional digital plesiosaur models, our results demonstrated that neck elongation does not noticeably affect the force of drag experienced by forward swimming plesiosaurs. Thicker necks did reduce drag compared with thinner necks, however. The consistent drag coefficient experienced by the three neck lengths used in this study indicates that, at least for forward motion at speeds from 1-10m/s, hydrodynamic implications were not a limiting selective pressure on the evolution of long necks in plesiosaurs. We also tested the effects of bending the long neck during forward motion. Bending a plesiosaur neck evenly in lateral flexion increased the surface area normal to flow, and subsequently increased drag force. This effect was most noticeable in the longest necked forms.

INTRODUCTION

Plesiosaurs are iconic extinct marine reptiles from the Mesozoic (Ketchum and Benson, 2010; Benson et al., 2012) exhibiting a great variety of neck lengths (Carpenter, 1999; O'Keefe, 2002; Kubo et al., 2012; Sachs et al., 2013; O'Gorman and Fernandez, 2016; Otero, 2016; Soul and Benson, 2017). For example, elasmosaurids were the most extreme taxa with neck lengths of up to 7m long – 63% of the total body length (Kubo et al., 2012). The body proportions of plesiosaurs mainly vary in skull sizes and neck lengths (O'Keefe and Carrano, 2005), and previous studies have shown that relative neck length of plesiosaurs increased over evolutionary time in elasmosaurids and microcleidids (Welles and Bump, 1949; Welles, 1952; Benson et al., 2012; Knutsen et al., 2012). Neck elongation evolved in many groups, from as early as the Late Triassic (in non-plesiosaurian pistosaurians), but occurred in most extremely form among Cretaceous elasmosaurids (Kubo et al., 2012). The selective pressures driving this evolution of ever longer necks are unclear, though several hypotheses regarding functional adaptations for feeding strategies have been proposed (Taylor, 1981; Callaway and Nicholls, 1997; McHenry et al., 2005; Zammit et al., 2008; Wilkinson and Ruxton, 2012; Noè et al., 2017). For nearly 200 years (Conybeare, 1824), illustrations and restorations of plesiosaur necks have been subject of imaginative reconstructions of what these animals might have looked like during life, and how their necks would have functioned (Rudwick, 2008).

The energetic cost of having a thicker neck would be reduced as the drag would be reduced. A study by Rothschild and Storrs (2003) found evidence of decompression

syndrome in plesiosaur humeri and femora which could indicate a deep-diving lifestyle. Decompression syndrome (also called avascular necrosis) is a pathology which includes the lack of blood supply to the bone and the bone tissue eventually dies (Rothschild, 1982). Avascular necrosis has been documented in mosasaurs and in some extinct marine turtles (Rothschild, 1987; Rothschild and Martin, 1987; Rothschild, 1991). The evidence of decompression syndrome in plesiosaurs proposes the possibility of viewing at least some plesiosaurs more as long-necked dolphins instead of the old-fashioned serpentine way they have been illustrated previously (Zarnik, 1925; Shuler, 1950; Rudwick, 2008). The fatter neck would also mean more insulation and thus greater tolerance of colder waters at depth in the water column.

Soft Tissue in Plesiosaurs

Soft tissue reconstruction of fossil organisms is clearly of importance when making paleobiological inferences, particularly concerning the ecology and lifestyle of extinct animals (Witmer, 1995). However, this is difficult as three-dimensional soft tissue preservation is extremely rare in the vertebrate fossil record. While there have been many ichthyosaurs preserved with carbonaceous skin outlines (e.g. Martin et al., 1986), the same is not the case for plesiosaurs. Nevertheless, two plesiosaur specimens have been discovered with what has been interpreted as preserved soft tissue (Frey et al., 2017; Vincent et al., 2017). The short-necked plesiosaur described by Frey et al. (2017) is preserved in ventral view and shows subdermal dorsal skin tissue, especially in the caudal region and between the ribs. Additionally, the long-necked plesiosaur described by Vincent et al. (2017) is preserved in lateral view and includes dark-coloured structures of different material around

the neck, hind flippers and tail. The structures identified as soft tissue around the neck extend around 2-3cm from the cervical vertebrae, indicating a thicker neck compared with the specimen described by Frey et al. (2017). This specimen indicates that we might have to re-evaluate our understanding of plesiosaurs with some being morphologically more akin to seals and sea-lions than the traditional reconstructions with a serpentine neck.

Hydrodynamics

Hydrodynamics is the study of moving fluids that are practically incompressible, and in the context of swimming performance has been explored for various aquatic taxa including extant marine mammals (Fish and Rohr, 1999; Fish et al., 2008; Segre et al., 2016), extant and extinct fish (Lauder and Madden, 2006; Borazjani and Sotiropoulos, 2010; Fletcher et al., 2014; Kogan et al., 2015; Van Wassenbergh et al., 2014, 2015; Fish and Lauder, 2017), and leatherback turtles (Dudley et al., 2014).

Any solid, such as a plesiosaur, moving through a fluid is subject to drag – a mechanical force on the object acting in the direction of fluid flow (Vogel, 2013). In fluid dynamics, drag can be divided into two types: pressure drag and skin-friction drag, where pressure drag is a function of body shape and friction-drag is dependent on surface area (Hoerner, 1965). For a streamlined body, at moderate to high Reynolds numbers, pressure drag is reduced due to the body shape (Hoerner, 1965). Friction drag increases with body size and the viscous forces acting on the surface of the body also increase with velocity (Hoerner, 1965; Vogel, 1989; McGowan, 1999). The plesiosaur models used in this study all exhibit the same body size, with variations in neck length. Friction drag is therefore negligible as the variation in neck length will only have a minor effect on friction drag.

Modern streamlined aquatic animals, such as fish, sea lions and cetaceans experience low pressure drag, making them well adapted for moving through water (Feldkamp, 1987; Fish and Rohr, 1999; Fletcher et al., 2014). As extant fully aquatic animals do not exhibit long necks, we are lacking a good living model for plesiosaur hydrodynamics. Several studies have explored and discussed the possible swimming ability and speed of plesiosaurs (Conybeare, 1824; Hutchinson, 1893; Andrews, 1910; Watson, 1924; Shuler, 1950; Taylor, 1981; Massare, 1988, 1994; Halstead, 1989; Bakker, 1993; O'Keefe, 2001; Motani, 2002; Henderson, 2006; Long et al., 2006; Carpenter et al., 2010; DeBlois, 2013; Liu et al., 2015; Muscutt et al., 2017). However, none of the previous studies have focused specifically on the locomotory implications of the neck, instead tending to focus on flippers and manoeuvrability.

Turning Performance

The understanding of the relationship between morphology and locomotor performance continues to be a dominant theme in biomechanics (Vogel, 2013). In aquatic locomotion, the two key components involved are hydrodynamic stability and turning ability (Stevens *et al.,* 2018). The energetic costs of swimming can be reduced by increasing stability, whereas avoiding and capturing prey is facilitated by turning performance (Stevens *et al.,* 2018). As animals rarely move continuously in straight lines (Fish and Rohr, 1999), it is obvious that turning performance holds a central part in the fundamental understanding of locomotor performance of animals. Turning performance has been investigated in great detail in many extant aquatic vertebrates (e.g. Walker, 2000; Drucker and Lauder, 2001; Alexander, 2003; Fish, 2002; Weihs, 2002; Fish *et al.,* 2003; Maresh *et al.,* 2004; Rivera *et al.,* 2006; Cheneval *et al.,* 2007; Fish *et al.,* 2008; Pierce *et al.,* 2011; Segre *et al.,* 2016; Clifton and Biewener, 2018; Stevens *et al.,* 2018), and is typically evaluated by two

metrices: manoeuvrability and agility (Stevens *et al.,* 2018). Manoeuvrability is normally measured as the space required to execute a turn, whereas agility is the rate of turning. Trade-offs between high stability and high turning performance are common (Van Wassenbergh *et al.,* 2014; Stevens *et al.,* 2018), and animals living in complex environments often tend to have high turning performance but low stability (Walker, 2000). In contrast, migratory animals are often highly stable but possess poor turning performances (Fish, 2002). Based on mechanical principles, animals with compact bodies are expected to be able to turn in tight spaces, whereas elongate bodies would be expected to enhance stability by helping to resist turning moments (Walker, 2000). Determining the bending effects of the long necks in plesiosaurs could help explore the ecology of plesiosaurs, and by combining such knowledge with hydrodynamics of plesiosaur flippers and neck flexibility will allow us to understand the possible feeding strategies in long-necked plesiosaurs.

Computational Fluid Dynamics

Used widely in engineering, Computational Fluid Dynamics (CFD) is a method that has been applied for several decades (e.g. Evans and Harlow, 1957; Harlow and Welch, 1965) and is essentially an *in silico* version of testing a physical model in a wind tunnel or flow tank. CFD is, in general, a numerical approach to solve the flow governing equations using computers. The governing equations, namely continuity and Navier-Stokes, relate velocity components and pressure of fluid flow. The system of equations is highly coupled and nonlinear, making analytical (exact) solutions of the governing equations difficult. In fact, the exact solutions are available only for a very few laminar flows in simple geometries. However, the rise of fast computers has allowed these equations to be extensively used in

simulations in an engineering context. CFD requires information on size, speed, and shape of an object to create a simulation that can help identify how the flow of a fluid responds to an object (Versteeg and Malalasekera, 2007).

The present study aimed to explore hydrodynamic changes associated with variations in neck length and thickness in plesiosaurs. First, we asked if longer necks affected overall drag of plesiosaurs during forward motion with straight and bent necks relative to shorter necks. Secondly, we wanted to test if drag was altered by a thicker neck compared to a thinner neck. Thirdly, we asked what the drag coefficients for the frontal forces and lateral forces was for plesiosaurs swimming with bent necks. Finally, we wanted to evaluate how the answers to the above questions affect existing hypotheses of what the neck was used for.

MATERIALS AND METHODS

Selected Plesiosaur Species

Our CFD simulations involved creating idealised plesiosaur models around which to simulate flow. By idealised we mean a model closely resembling a real-life plesiosaur concerning body outline and volume. For the three neck lengths, three plesiosaur species were chosen as a basis for neck proportions. Total body length for the species chosen included the distance from the tip of skull to the end of tail. For the long-necked model, *Albertonectes vanderveldei* (73.5 Ma) was chosen as it is the plesiosaur with the longest neck found to date (7 m neck and 11 m in total: Kubo et al., 2012), *Muraenosaurus leedsii* (162 Ma) was used for the intermediate-necked model (2.5 m neck and 6 m in total:

Andrews, 1910), and *Meyerasaurus victor* (182 Ma) for the short-necked model (0.7 m neck

and 3.35 m in total: Smith and Vincent, 2010). As these three species have very different

neck lengths, and are from three different plesiosaur families (elasmosaurids, cryptoclidids,

and rhomaleosaurids, respectively), they provide a range of plesiosaur morphologies to

model.

Modelling the Plesiosaur

The first 3D model was created based on *M. victor* (see below) and then the neck was

scaled in length to match the neck:body ratios of *M. leedsi* and *A. vanderveldei*. All models

had identical frontal area. The percentage of neck length of the total body length was 21%

for the short-necked, 42% for the intermediate-necked, and 64% for the long-necked

plesiosaur model. The intermediate-necked plesiosaur model was used as a template for the

thick- and thin-necked plesiosaur simulations.

To create the plesiosaur base model a ventral view (Fig. 1A-B) of the short-necked

plesiosaur species (Smith and Vincent, 2010) was imported into Autodesk Maya. The image

was scaled accordingly and used as a basis for modelling the 3D plesiosaur. First, the body

was formed using Non-Uniform Rational Basis Spline (NURBs) circles created along the

length of the plesiosaur and scaled accordingly in the parts of the plesiosaur body changing

in size (Fig. 1A-B). All circles were selected and lofted to form a solid volume (Fig. 1C-D),

a method previously employed by Bates et al. (2009a; 2009b; 2012) and Hutchinson et al.

(2011) on dinosaurs. NURBs are used when working with highly flexible shape modelling

formats and can be used to produce anything from simple 2D geometry shapes (e.g.

parabolic curves, circles, and ellipses) to complex 3D free-form curves (Bates et al., 2009b).

In Autodesk Maya, 'cubic' interpolation was used to loft between the circles to ensure smoothness to the transition of each circle resulting surface. To make the model watertight, the anterior- and posterior-most parts were 'capped' with two tiny (i.e. not visible) planar end surfaces. The flippers were formed using the same approach, with additional rotation to the circles to place them correctly relative to the body of the plesiosaur. Flippers were modelled on one side of the plesiosaur and duplicated and mirrored for the opposite side. The model was then straightened by aligning the NURBs circles forming the neck, body, and tail to the Y-axis. The flippers were rotated 10 degrees down from the horizontal plane (Fig. 1E).

For the intermediate- and long-necked plesiosaur models the neck part of the short-necked model was extended according to the neck/body ratio above. For the thick-necked plesiosaur model, the NURBs circle at the base of the neck was increased in size until it equalled the most anterior body circle, creating a smooth transition. This increase in circle size, 343% cervical width, was then applied to the NURBs circles making up the rest of the neck. Conversely, the thin neck was produced by shrinking the NURBs circles making up the neck until they touched the outlines of the cervical vertebrae (i.e. each NURBs circle diameter was equal to 100% cervical width). All models were exported as IGES surface files.

The three thin-necked plesiosaur models were also simulated with the necks laterally curved. Joints between each pair of cervical vertebrae were inserted midway between each NURBs circle. The models had one extra joint attached in the posterior end of the head in order to have a smooth bending transition from head to neck. Each joint was paired by parenting the joint to the respective cervical using 'NURBs circles' along the neck. By parenting each joint to its respective NURBs circle the two objects were associated with one

another making the number of all joints and NURBs circles more organised. This way the rotation and translation information for each pair (joint + NURBs circle) followed the adjacent joint and circle (Fig. 2). The neck lengths were used to calculate the distance between each joint, by dividing the total neck length with the number of cervical vertebrae for the given species. The short-necked model was 0.8 m in neck length, and with a total number of 28 joints; a joint was positioned at every 0.03 m. For the intermediate model the neck length was 2.0 m and a total of 42 joints were inserted, at every 0.048 m. For the long-necked model 76 joints were inserted in the neck, one at every 0.058 m, making a total neck length of 4.4 m. After insertion of joints in the neck region of the plesiosaur models the necks were bent laterally into four different poses (total neck curvature: 22.5°, 45°, 67.5°, and 90°). Lateral rotation was chosen because turning in the horizontal plane (rather than diving or rising through dorsal/ventral flexion) ignores effects of buoyancy, i.e., lateral flexion required no prior knowledge of whether plesiosaurs moved up- or downwards in the water column. Each joint in the neck of the three idealized plesiosaur models was equally rotated, distributing the curvature over the entire length. Rotations between necks of different length and cervical count were made consistent by dividing total desired rotation by the number of cervical vertebrae and rotating each joint by that number (Fig. 2B). The specific rotations required between each vertebra/joint to reach the four poses of neck bending are shown in Table 1 and calculated by dividing bend angle by the number of joints. The five poses for each model are shown in Figure 3. At very small rotations between each vertebra a large whole-neck rotation is achieved. The plesiosaur models were saved individually in IGES format after each rotation was entered in Autodesk Maya.

Computational Fluid Dynamics Simulations

The 3D models were individually imported to Autodesk Simulation CFD (version 2017 and 2018) where the simulations of water flow around the plesiosaur models were undertaken. Simulations were based on the RANS approach using the turbulence model k-epsilon (Rahman, 2017). The external boundaries of the computational domain over which the governing equations are solved consisted of a 25m cube with one face in front of the plesiosaur model defined as an inlet, where water velocity was specified in m/s. The opposite face of the cubic domain, located posterior to the plesiosaur, was defined as an outlet boundary condition (zero pressure gradient across the boundary). Mesh and domain independence studies have been undertaken to determine the appropriate mesh size and computational domain of the models. As a result, the mesh size and domain were set to 0.01m and 1.0m, respectively. A cuboid region of refinement with mesh size of 0.5m was applied to the computational domain surrounding the plesiosaur model in order to capture the wake, resulting from the relative motions of fluid and plesiosaur (Fig. 1F). An additional cuboid region of refinement with mesh size of 0.05m was applied to the computational domain surrounding the neck region of the plesiosaur models with bent necks to improve resolution even further around the neck region.

In all cases, 3D incompressible water flow was simulated with the plesiosaur models held stationary. This is computationally simpler than moving the animal through a stationary fluid because it does not require remeshing; however, the physics is effectively identical. Flow-stream velocities of 1, 3, 5, 7 and 10 m/s (for Reynolds numbers see supplementary data; total body length of plesiosaur models and free-stream velocity have been taken as the characteristic length and velocity, respectively, to calculate Re_x) were simulated for all five straight-necked plesiosaur models. The plesiosaur models with bent necks were simulated at 1, 5 and 10 m/s. The velocities were chosen because the swimming speeds of long-necked

plesiosaurs have been proposed to be within this range depending on when the plesiosaur would use its sustained swimming speed (2.17-2.51 m/s in Massare, 1988, and 3.8-4.0 m/s in Massare, 1994). Note however that Massare (1988) showed these calculated speeds were likely too high – hence our use of speeds lower than 4.0 m/s. Data for modern cetaceans typically falls towards the lower end of our range. For example, speeds of 2.2-2.8 m/s are typical for smaller dolphins, although Orcas (*Orcinus orca*) have sprint speeds in excess of 8.3 m/s (Wilson and Mittermeier, 2014). We simulated velocities up to 10 m/s to see how/if flow velocity patterns and the drag coefficient would change dramatically at very high speeds. The results were visualised as two-dimensional cross sections of flow velocity magnitude, and in isometric view with flow streamlines (cylinders). The drag force was calculated by Autodesk Simulation CFD to quantify flow around the digital reconstructions of plesiosaurs, and drag coefficients were manually calculated using the frontal area of the plesiosaur models.

The Reynolds numbers used in this study were in the turbulent flow range (see supplementary data). Consequently, we used the turbulence model k-epsilon based on pre-studies (see supplementary data) on reference shapes of a sphere and cylinder model to allow comparison with data from Vogel (1989).

For the present study the characteristic length of the plesiosaur models could be determined as either total body length or trunk length. If Reynolds numbers are a crucial part of the study, it is important to consider whether to use the total body length or the trunk length of the animal. This is because the Reynolds number will be the same for all five models in case of using trunk length as characteristic length. In addition, the total body length will change the Reynolds number depending on which model is the case of study, which can also be observed from Table S1 (Supplementary Data 1). Bending the neck of the

plesiosaur models will technically affect the characteristic length of the body as it decreases normal to the flow, and the Reynolds number will decrease as well. However, the Reynolds number was not used for further analysis in this study and the characteristic length is thus based on each model with the neck held straight.

RESULTS

Straight Neck

Visually our simulations showed the flow velocity following the hydrodynamic body of the plesiosaur models with areas of low velocity in the areas behind the flippers and tail regions (Fig. 4A-E). Additionally, areas of low velocity were observed around the neck for especially the long-necked model (Fig. 4E). In the rest of the models the low velocity area in the neck region was only detectable on the lateral sides of the neck. The thin-necked model showed a strong difference in water pressure towards the frontal part of the flippers (up to 200 pa) and less pressure around the head (down to 100 pa) compared with the thick-necked model (Fig. 4F).

Consistent with theoretical expectations, our simulations showed that with increasing velocity, higher drag coefficients were experienced by the plesiosaur models of all three different neck lengths. The thin-necked plesiosaur model showed little difference in velocity and drag force patterns from the intermediate neck (Fig. 5). However, the thick necked plesiosaur model was observed exhibiting a generally lower drag coefficient noticeably above speeds of 5-10 m/s (Fig. 5). The relative difference in percent in drag coefficient

between the thick and thin-necked models was 17% at 5m/s, 16% at 7m/s and 18% at 10m/s, so the thicker neck saw a drag reduction of 15-20% compared with the thin-necked model.

Bent Neck

When comparing drag coefficients for the idealized plesiosaur models, the short-necked model experienced the least drag, and the long-necked experienced the most drag (Fig. 6-7). All three models demonstrated a nearly linear relationship in the increase of drag for bending of 45° – 90° at all three velocities (Fig. 6). As was expected the drag was highest for the long-necked model, and the least for the short-necked model with the intermediate neck being between the two. The lateral drag forces experienced to the left side all three models peaked in drag at 67.5° and decreased slightly from 67.5° – 90°, with the highest drag force seen in the long-necked model and the least in the short-necked model with the intermediate neck being between the two (Fig. 7). Drag was generally a lot higher for the long-necked model (Fig. 6-7: blue lines) compared with the short- (Fig. 6-7: red lines) and intermediate (Fig. 6-7: green lines) necked model. The drag was almost the same for all three models until around 22.5° and diverges thereafter for the long-necked model, with a higher increase compared with the short- and intermediate-necked model. There was an increase of four orders of magnitude in drag from 1 m/s – 10 m/s for all three models, and three orders of magnitude from 1 m/s – 5 m/s.

The flow velocity patterns at 1, 5 and 10 m/s were clearly different for the short-, intermediate and long-necked idealized plesiosaur models when the necks were bent 90°. At 5 m/s and 10 m/s the flow velocities were almost identical for all three neck lengths. The long-necked model experienced a relatively larger area of low flow velocity at all three flow

velocities in the path behind the neck (Fig. 8A-C). The flow velocity patterns in the wake behind the three plesiosaur models showed that the velocity here decreased, especially behind the flippers and in the tail region.

The pressure experienced towards the bent neck in the direction of flow was visibly different for the three neck lengths. The area of increased pressure on the neck covered most of the neck length for the short-necked plesiosaur model and about 2/3 of the intermediate-necked plesiosaur model, whereas for the long-necked plesiosaur model only half of the neck length had an area with increased pressure (Fig. 8D). The least pressure was seen around the flippers and the backside of the bended neck for all three plesiosaur models.

DISCUSSION

Neck Elongation and Thickness

We found that elongation of the neck had little effect on the hydrodynamics when held completely straight (Fig. 5). However, it is qualitatively obvious that the longer the neck is the more drag it will experience if not held completely straight (see discussion below). Making manoeuvres in the water, such as flexing the neck, would almost certainly have required more muscular strength than what would be available to the animal (Noè et al., 2017), so plesiosaurs swimming with straight necks is likely in cases where the animals would have to approach prey fast over a short distance. Here the animals would benefit from reduced energy costs to a minimum in order to keep the speed steady, and therefore having

nearly straight necks when swimming. In addition, an animal swimming any distance would use less energy overcoming drag if the neck was straight – as suggested by our simulations.

The long-necked plesiosaur model experienced higher forces of drag the more the neck was bent, compared with the short- and intermediate-necked models. The drag coefficient in the direction of flow was the same for all three models at all three speeds until a neck bending angle of around 22.5° and diverges thereafter. This was because longer neck produced a greater frontal area when bent compared to the short- and intermediate-necked models. Looking at the lateral drag force (Fig. 1F negative Z-direction of the 3D coordinate system.) all three models experienced different amounts of drag at all degrees of bending (Fig. 7). At all three speeds, the intermediate-necked model experienced slightly more than double the amount of drag compared with the short-necked model, and for the long-necked model drag almost tripled compared with the intermediate-necked model. We can see from the drag coefficients that extreme bending of the neck would have had major consequences during forward motion at moderate to high velocities. At lower angles of neck bend (0-45°) plesiosaurs with various neck lengths would be able to turn their necks sideways without creating high amounts of drag, which could indicate that plesiosaurs could possibly have fed on prey using a strategy where the neck would move sideways in order to capture prey close to it.

The amount of pressure towards the part of the bent neck exposed by the water flow at 5 m/s was different for the three neck lengths as the area of the neck exposed to the flow was different in size. The short-necked model was exposed to high amounts of pressure towards most of its neck, the intermediate-necked model was exposed to the pressure for about 2/3 of its neck, and the long-necked model only had great amounts of pressure pushing towards the anterior-half of the neck.

The CFD simulations also indicate that neck thickness had a noticeable effect on the amount of drag force and water pressure generated by the plesiosaur, with the most water pressure happening when the plesiosaur model was reconstructed with thinnest neck length, and the largest wake size and highest drag force occurring with the shortest and thinnest neck length (Fig. 5). Note however, that the change in wake size and drag force was only apparent for water velocities above 5.0 m/s. This would be a speed substantially faster than typical for a small dolphin (see above). Drag forces experienced by the plesiosaur models were similar across different neck lengths, though longer necks experienced slightly less overall drag force. The largest reduction in drag at any given speed was observed in the thick-necked model (Fig. 5).

The thickness of plesiosaur necks has been a longstanding difficulty in reconstructing the life appearance of these animals, with both thin- and thick-necked plesiosaurs being illustrated in the past (Cope, 1869; Zarnik, 1925; Welles, 1943; Welles and Bump, 1949; Shuler, 1950; Rudwick, 2008). A thin neck would, according to our results, have been a disadvantage for the plesiosaur during locomotion as it would have created more drag force and water pressure in comparison to a thicker-necked plesiosaur, especially if the animal was moving quickly.

The soft tissue preservation found in fossils can help us understand how extinct animals would appear and move, as the muscles form an integral part of the anatomy and play a fundamental role in feeding, locomotion and other physiological activities (Witmer, 1995; Lautenschlager, 2017). If the soft tissue is taken into account it allows us to justify a certain ecology and phylogeny for a given animal (Witmer, 1995). Although many plesiosaurs are found complete and fully articulated there is still an absence of soft tissue preserved throughout the Plesiosauria clade (O'Keefe, 2001; Frey et al., 2017), making it

difficult to interpret their ecology and paleobiology. The specimen described by Vincent et al. (2017) is covered with more soft tissue around the neck compared with the specimen reported by Frey et al. (2017). The two specimens discussed by Frey et al. (2017) and Vincent et al. (2017) have two different neck lengths. Combining the difference in neck thickness among the two plesiosaur specimens with the results from the present study suggests that short-necked plesiosaurs would have benefited more from slender necks (if that was the case in reality) than the long-necked species. However, more plesiosaur specimens including soft tissue are required to clarify whether plesiosaurs had thick or thin necks.

In addition to soft tissue, bite marks have also been found in various plesiosaur bones. With only one exception known (Sato et al., 2006), the bite marks observed in plesiosaur bones occur on humeri and flippers (Forrest and Oliver, 2003; Everhart, 2005; Sato et al., 2006), which might suggest that plesiosaurs had thick necks. Having a thicker neck makes it harder for predators to leave bite marks on the actual vertebrae, especially the neck vertebrae. Thicker necks would therefore reduce the likelihood of finding cervical vertebrae with healed bite marks, as any bite deep enough to reach the vertebrae would likely be fatal. However, again we need more plesiosaur specimen observed with bite marks in vertebrae to clarify that plesiosaurs had thin necks.

Turning Performance

The streamlined bodies of many aquatic vertebrates represent a balance between stability and manoeuvrability in locomotion. This balance has been extensively studied in extant aquatic vertebrates, such as pinnipeds (Fish et al., 2003; Cheneval et al., 2007; Pierce et al., 2011), cetaceans (Fish, 2002; Maresh et al., 2004; Fish et al., 2008), turtles (Rivera et

al., 2006; Stevens et al., 2018), fish (Drucker and Lauder, 2001; Weihs, 2002), and diving birds (Clifton and Biewener, 2018).

The unique and iconic morphology of plesiosaurs makes it difficult to make inferences about stability and manoeuvrability based on extant taxa. Plesiosaurs, as far as we can tell from the fossil record, did not have a fluke to generate thrust or for steering their bodies in the water like cetaceans. Nor did they seem able to tuck their necks in, as penguins do, in order to avoid creating more drag. Therefore, plesiosaurs might have used a combination of the flippers and head/neck movement to turn their bodies (and eventually necks) slowly to avoid high energy costs.

The radius of the space used in turning the neck was greater for the long-necked plesiosaur model and least for the short-necked plesiosaur model, making relatively short-necked plesiosaurs more manoeuvrable compared with longer-necked forms due to the smaller turning path and higher neck flexibility (Walker, 2000). When a plesiosaur turns its neck, it would go from travelling forward, bending its neck and then make the actual turn. As in sea lions (Cheneval et al., 2007), the speed of travel when swimming forward would eventually have to be reduced in order to turn the neck and body due to the forces, torques and momentum involved.

Momentum is equal to mass times velocity (Alexander, 2003), and therefore it is dependent on the amount of water moved when a plesiosaur moves forward or turns (O'Keefe and Carrano, 2005). The necks of plesiosaurs are a relatively small proportion of overall mass, thus long-necked plesiosaurs would have to move only a slightly larger volume of water compared with shorter-necked forms. The energy-cost needed to combat

momentum when changing direction would therefore be marginally higher in the long-necked plesiosaurs.

Ecology and Behaviour of Plesiosaurs

Wilkinson and Ruxton (2012) proposed long necks in most cases could be explained in terms of foraging requirements. A long neck must be at least somewhat flexible in order to confer a benefit to foraging, either by increasing the feeding envelope, or by increasing manoeuvrability acting as a steering apparatus. Indeed, in extant aquatic animals like sea lions, we see flexion in the neck region as the animals turn in the water (Fish et al., 2003; Cheneval et al., 2007). Previous studies have suggested that plesiosaurs had some extent of flexibility along the neck (Zarnik, 1925; Evans, 1993; Zammit et al., 2008; Noè et al., 2017). Furthermore, the fused atlas-axis complex in plesiosaurs could provide cranial movement due to the cup-shaped occipital bone (VanBuren and Evans, 2016) allowing the plesiosaur to scan for possible prey more efficiently. Plesiosaurs would presumably have benefited in terms of foraging by using a combination of the long necks, manoeuvrability of the head, and thrust from the flippers to pursue and capture prey.

The flexibility of a plesiosaur neck determines how fast the animal can manoeuvre when trying to escape predators or search for prey. Based on the previous studies on range of motion in plesiosaur necks (Welles, 1943; Evans, 1993; Zammit et al., 2008; Nagesan et al., 2018), the neck appears to have been relatively inflexible, at least for short-necked forms. Given the drag coefficients calculated here, this seems to have been particularly important when swimming at higher speed (>5m/s). The higher number of neck vertebrae would logically create more flexibility in long-necked forms (e.g. elasmosaurids and

microcleidids), even if individual intervertebral rotations were small. However, long-necked forms achieved neck elongation both through increasing the number of cervical vertebrae and increasing the length of individual cervical vertebrae relative to vertebral width and height (Buchholtz and Schur, 2004; O'Keefe and Hiller, 2006). These longer vertebrae also generally had closely fitting neural spines (Kubo et al., 2012), which in combination with longer vertebrae may have acted to restrict flexibility and stiffen the neck, relative to short-necked forms. Relatively short-necked forms have more space between each neural spine (Sachs et al., 2016) as well as relatively shorter centra (Smith and Araújo, 2017), creating space for higher flexibility (Evans, 1993). It is likely, therefore, that plesiosaurs exhibited a range of feeding strategies that varied with neck length and stiffness, and swimming performance (Massare, 1988, 1994; O'Keefe, 2001; Motani, 2002; Carpenter et al., 2010).

The potential feeding envelope of an animal is affected by its ability to manoeuvre its head via the neck. The feeding envelopes of the three plesiosaur models with respective arc lengths are visualised in Figure 9, showing a clear difference between the three models in both area and arc length. The arc length for the three feeding envelopes would be around 2.22 m for the short-necked model, 3.83 m for the intermediate-necked model, and 7.93 m for the long-necked model. Having a relatively long neck would mean that long-necked plesiosaurs would have a larger foraging area compared to shorter-necked forms (Fig. 9). Comparing with extant long-necked vertebrates, such as ostriches, camels and giraffes, the lateral feeding envelope is stretched over a larger area compared with plesiosaurs, due to the slightly higher amounts of lateral flexibility at the base of the neck found in ostriches, as well as camels and giraffes (Dzemski and Christian, 2007). This increased feeding envelope would be equally applicable if plesiosaurs acted as floating feeding stations, extending the neck beneath the body (Noè et al., 2017).

Noè et al. (2017) recently stated that manoeuvrability in plesiosaur necks would be affected by drag generated by the length of the neck, which would be greater than the muscular strength in the neck. Our high drag forces on the long-necked plesiosaur model with bent neck support this. Due to the physical restrictions in turning the neck, shorter-necked plesiosaurs would likely have turned at relatively higher speeds than long-necked forms. Short-necked plesiosaurs would therefore have been more efficient at grabbing their prey quickly than long-necked plesiosaurs.

The long neck in plesiosaurs was clearly a successful adaptation, as shown by their long evolutionary history (Smith, 2007). However, it has been demonstrated that there were multiple evolutionary reductions of neck length within the Elasmosauridae (Serratos et al., 2017), and pliosaur morphotypes were able to evolve independently in more than one clade (O'Keefe, 2002; Druckenmiller and Russell, 2008; Ketchum et al., 2010; Benson and Druckenmiller, 2014; Soul and Benson, 2017). Our results show that having a long neck would not necessarily be a hydrodynamic disadvantage as the neck length did not affect the drag force added on to the plesiosaur model (Fig. 5). It was, however, likely a foraging advantage, and may have been a driver of diversity, enabling exploitation of new foraging strategies.

Plesiosaurs have been considered as both relatively slow (Conybeare, 1824; Andrews, 1910; Watson, 1924; Shuler, 1950; Taylor, 1981; Massare, 1988, 1994) and fast swimmers (Hutchinson, 1893; Halstead, 1989; Bakker, 1993). To avoid the energetic cost of high amounts of drag, plesiosaurs might have evolved thicker necks to allow effective hunting strategies like ambushing prey – fast acceleration of the body over a short distance. Therefore, it is more reasonable that plesiosaurs had a variety of swimming speeds in accordance with neck length, as suggested by Massare (1994), instead of being labelled as

either fast or slow swimmers. Our results indicate that thicker necks reduced drag, which lends support for a more expanded neck than is traditionally incorporated into reconstructions.

CFD as a Tool

Through three-dimensional (3D) numerical simulations we can study fossils in more detail without damaging the specimens studied (Sutton et al., 2017). The rapidly developing methods in virtual paleontology can help us visualise and analyse fossils digitally much easier and quicker than previously, and the methods have changed the way we study fossil specimens (Davies et al., 2017). CFD is one of many ways to perform virtual paleontology and is a relatively inexpensive method to visualise hydrodynamic flow modelling in 3D (Sutton et al., 2017) and has been used for several types of studies in paleontology (Liu et al., 2015; Rahman et al., 2015a, 2015b; Dynowski et al., 2016; Rahman, 2017; Rahman and Lautenschlager, 2017) and biology (Dudley et al., 2014; Van Wassenbergh et al., 2014, 2015; Kogan et al., 2015; Beckert et al., 2016; Bradney et al., 2016; McHenry et al., 2016). Thus, CFD has become an important tool in understanding flow dynamics and in helping interpret the ecology and biology of aquatic animals and plants, especially in extinct forms due to lack of modern analogues. In our study CFD-RANS has helped answer simple locomotory questions concerning the functional morphology and hydrodynamics of plesiosaur necks. An extension of the present study could include more computationally intensive models with additional variables tested such as surface of the models, variances in density and trunk volume, etc. Thus, more studies in this field are required to understand the complexity in the lifestyle of plesiosaurs.

CONCLUSIONS

We used CFD-RANS to study the functional morphology and hydrodynamic implications of plesiosaur necks. A thick-necked plesiosaur would have a hydrodynamic advantage compared with a thinner-necked plesiosaur, however, these effects are only seen at velocities which may be faster than was typical (or even possible) for most plesiosaur species. Broader necks reduce the surface area normal or near normal to flow direction, and thus reduce pressure drag. This suggests that any plesiosaurs using a pursuit hunting strategy may have been under selection pressure to evolve a thicker neck. The consistent drag force experienced by the three neck lengths used in this study indicated that, at least for straight forward motion, hydrodynamic implications were not a limiting selective pressure on the evolution of long necks in plesiosaurs. Massare (1994) found that long-necked plesiosaurs did experience increased drag, and therefore suggested slower swimming speeds and different foraging strategies for the long-necked plesiosaurs compared with short-necked plesiosaurs. In contrast, the present study suggests that short- and long-necked plesiosaurs did not vary greatly in drag experienced during forward locomotion. Given the long survival of the plesiosaurian body plan in the geological record, it is not surprising that the quantitative results from the present study support the notion that the long neck was not particularly disadvantageous hydrodynamically. In conjunction with soft-tissue preservation reported in plesiosaur necks, our simulations provide support for reconstructing plesiosaurs with more sea lion-like neck morphology than they have traditionally been reconstructed with.

This study also looked at the biomechanical implications for plesiosaurs with short, intermediate and long necks laterally flexed. The hunting styles of plesiosaurs would likely have been quite diverse. If plesiosaurs with long necks attempted to turn their heads at high velocities, the physical restrictions (drag forces and torques) of manoeuvrability, and large turning radii, might have resulted in injury. Relatively short-necked plesiosaurs would be capable of turning faster than long-necked forms. This study and additional research will hopefully help to shed light on the biomechanical implications of the long neck in plesiosaurs, and more broadly inform hypotheses concerning the lifestyles and evolutionary history of plesiosaurs.

ACKNOWLEDGMENTS

LITERATURE CITED

Alexander, R. M. 2003. Principles of Animal Locomotion. Princeton University Press, Princeton and Oxford, 385pp.

Andrews, C. W. 1910. A Descriptive Catalogue of the Marine Reptiles of the Oxford Clay, Part I. British Museum (Natural History), London, 205pp.

Bakker, R. T. 1993. Plesiosaur extinction cycles—events that mark the beginning, middle, and end of the Cretaceous. Evolution of the western interior basin. Geological Association of Canada, Special Paper 39:641–664.

Bates, K. T., R. B. J. Benson, and P. L. Falkingham. 2012. A computational analysis of locomotor anatomy and body mass evolution in Allosauroidea (Dinosauria: Theropoda). Paleobiology 38(3):486–507.

Bates, K. T., P. L. Falkingham, B. H. Breithaupt, D. Hodgetts, W. I. Sellers, and P. L. Manning. 2009a. How big was 'Big Al'? Quantifying the effect of soft tissue and osteological unknowns on mass predictions for *Allosaurus* (Dinosauria:Theropoda). Palaeontologia Electronica 12(3):1–33.

Bates, K. T., P. L. Manning, D. Hodgetts, and W. I. Sellers. 2009b. Estimating mass properties of dinosaurs using laser imaging and 3D computer modelling. PLoS ONE 4(2):1–26.

Beckert, M., B. E. Flammang, E. J. Anderson, and J. H. Nadler. 2016. Theoretical and computational fluid dynamics of an attached remora (*Echeneis naucrates*). Zoology 119(5):430–438.

Benson, R. B., and P.S. Druckenmiller. 2014. Faunal turnover of marine tetrapods during the Jurassic-Cretaceous transition. Biological Reviews 89(1): 1–23.

Benson, R. B., M. Evans, and P. S. Druckenmiller. 2012. High diversity, low disparity and small body size in plesiosaurs (Reptilia, Sauropterygia) from the Triassic-Jurassic boundary. PLoS One 7(3):e31838.

Borazjani, I., and F. Sotiropoulos. 2010. On the role of form and kinematics on the hydrodynamics of self-propelled body/caudal fin swimming. Journal of Experimental Biology 213(1):89–107.

Bradney, D. R., A. Davidson, S. P. Evans, B. E. Wueringer, D. L. Morgan, and P. D. Clausen. 2016. Sawfishes stealth revealed using computational fluid dynamics. Journal of Fish Biology 90(4):1584–1596.

Brown, D. S. 1981. The English Upper Jurassic *Plesiosauroidea* (Reptilia) and a review of the phylogeny and classification of the Plesiosauria. Bulletin of the British Museum (National History), Geology Series 35(4):253–347.

Buchholtz, E. A., and S. A. Schur. 2004. Vertebral osteology in Delphinidae (Cetacea). Zoological Journal of the Linnean Society 140(3):383-401.

Callaway, J. M., and E. L. Nicholls. 1997. Ancient Marine Reptiles. Academic Press, 501 p.

Carpenter, K. 1999. Revision of North American elasmosaurs from the Cretaceous of the Western Interior. Paludicola 2(2):148–173.

Carpenter, K., F. Sanders, B. Reed, J. Reed, and P. Larson. 2010. Plesiosaur swimming as interpreted from skeletal analysis and experimental results. Transactions of the Kansas Academy of Science 113(1/2):1–34.

Chatterjee, S., and B. J. Small. 1989. New plesiosaurs from the Upper Cretaceous of Antarctica. Geological Society Special Publication 47:197–215.

Cheneval, O., R. W. Blake, A. W. Trites, and K. H. S. Chan. 2007. Turning maneuvers in Stellar Sea Lions (*Eumatopias jubatus*). Marine Mammal Science 23(1):94–109.

Clifton, G. T., and A. A. Biewener. 2018. Foot-propelled swimming kinematics and turning
 strategies in common loons. The Journal of Experimental Biology
 221(19):jeb168831.

Conybeare, W. D. 1824. On the Discovery of an almost perfect Skeleton of the *Plesiosaurus*.
 Transactions of the Geological Society of London 1:381–390.

Cope, E. D. 1869. Extinct Batrachia, Reptilia and Aves of North America. Transactions of
 the American Philosophical Society 14:1-252.

Davies, T. G., I. A. Rahman, S. Lautenschlager, J. A. Cunningham, R. J. Asher, P. M.
 Barrett, K. T. Bates, S. Bengtson, R. B. Benson, D. M. Boyer, J. Braga, J. A. Bright,
 L. P. A. M. Claessens, P. G. Cox, X. Dong, A. R. Evans, P. L. Falkingham, M.
 Friedman, R. J. Garwood, A. Goswami, J. R. Hutchinson, N. S. Jeffery, Z. Johanson,
 R. Lebrun, C. Martínez-Pérez, J. Marugán-Lobón, P. M. O'Higgins, B. Metscher, M.
 Orliac, T. B. Rowe, M. Rücklin, M. R. Sánchez-Villagra, N. H. Shubin, S. Y. Smith,
 J. M. Starck, C. Stringer, A. P. Summers, M. D. Sutton, S. A. Walsh, V. Weisbecker,
 L. M. Witmer, S. Wroe, Z. Yin, E. J. Rayfield, and P. C. J. Donoghue. 2017. Open
 data and digital morphology. Proceedings of the Royal Society B: Biological
 Sciences 284(1852):1–32.

Deblois, M. C. 2013. Quantitative Reconstruction and Two-Dimensional, Steady Flow
 Hydrodynamics of the Plesiosaur Flipper. Theses, Dissertations and Capstones, Paper
 501.

Druckenmiller, P. S. and A. P. Russell. 2008. A phylogeny of Plesiosauria (Sauropterygia)
 and its bearing on the systematic status of Leptocleidus Andrews, 1922. Zootaxa
 1863:1–120.

Drucker, E. G. and G. V. Lauder. 2001. Wake dynamics and fluid forces of turning maneuvers in Sunfish. The Journal of Experimental Biology 204:431-442.

Dudley, P. N., R. Bonazza, T. T. Jones, J. Wyneken, and W. P. Porter. 2014. Leatherbacks swimming in silico: modeling and verifying their momentum and heat balance using computational fluid dynamics. PLoS One 9(10):e110701.

Dynowski, J. F., J. H. Nebelsick, A. Klein, and A. Roth-Nebelsick. 2016. Computational fluid dynamics analysis of the fossil crinoid *Encrinus liliiformis* (Echinodermata: Crinoidea). PLoS One 11(5):e0156408.

Dzemski, G., and A. Christian. 2007. Flexibility along the neck of the ostrich (*Struthio camelus*) and consequences for the reconstruction of dinosaurs with extreme neck length. Journal of Morphology 268(8):701-714.

Evans, M. 1993. An investigation into the neck flexibility of two plesiosauroid plesiosaurs: *Cryptoclidus eurymerus* and *Muraenosaurus leedsii*, University College, London, 64 p.

Evans, M. W., and F. H. Harlow. 1957. The particle-in-cell method for hydrodynamic calculations (No. LA-2139). Los Alamos Scientific Laboratory Report.

Everhart, M. J. 2005. Bite marks on an elasmosaur (Sauropterygia; Plesiosauria) paddle from the Niobrara Chalk (Upper Cretaceous) as probable evidence of feeding by the lamniform shark, *Cretoxyrhina mantelli*. PalArch, Vertebrate paleontology series 2:14–24.

Feldkamp, S. D. 1987. Swimming in the California sea lion: morphometrics, drag and energetics. Journal of Experimental Biology 131:117–135.

Fish, F. E. 2002. Balancing requirements for stability and maneuverability in cetaceans. Integrative and Comparative Biology 42:85-93.

Fish, F. E., L. E. Howle, and M. M. Murray. 2008. Hydrodynamic flow control in marine

    mammals. Integrative and Comparative Biology 48(6):788–800.

Fish, F. E., J. Hurley, and D. P. Costa. 2003. Maneuverability by the sea lion *Zalophus*

    californianus: turning performance of an unstable body design. Journal of

    Experimental Biology 206:667–674.

Fish, F. E., and G. V. Lauder. 2017. Control surfaces of aquatic vertebrates: active and

    passive design and function. Journal of Experimental Biology 220:4351–4363.

Fish, F. E., and J. J. Rohr. 1999. Review of Dolphin Hydrodynamics and Swimming

    Performance. Space and naval warfare systems, San Diego CA, 187 p.

Fletcher, T., J. Altringham, J. Peakall, P. Wignall, and R. Dorell. 2014. Hydrodynamics of

    fossil fishes. Proceedings of the Royal Society B: Biological Sciences

    281(1788):20140703.

Forrest, R., and N. Oliver. 2003. Ichthyosaurs and plesiosaurs from the Lower Spilsby

    Sandstone Member (Upper Jurassic), north Lincolnshire. Proceedings of the

    Yorkshire Geological Society 54(4):1–8.

Frey, E., E. W. A. Mulder, W. Stinnesbeck, H. E. Rivera-Sylva, J. M. Padilla-Gutiérrez, and

    A. H. González-González. 2017. A new polycotylid plesiosaur with extensive soft

    tissue preservation from the early Late Cretaceous of northeast Mexico. Boletín de la

    Sociedad Geológica Mexicana 69(1):87–134.

Halstead, L. B. 1989. Plesiosaur locomotion. Journal of the Geological Society 146:37–40.

Harlow, F. H., and J. E. Welch. 1965. Numerical calculation of time-dependent viscous

    incompressible flow of fluid with free surface. Physics of Fluids 8(12):2182–2189.

Henderson, D. 2006. Floating point: a computational study of buoyancy, equilibrium, and

    gastroliths in plesiosaurs. Lethaia 39(3):227–244.

Hoerner, S. F. 1965. Fluid Dynamic Drag. Hoerner, Midland Park, New Jersey, 455 p.

Howland, H. C. 1974. Optimal strategies for predator avoidance: The relative importance of speed and manoeuvrability. Journal of Theoretical Biology 47(2):333-350.

Hutchinson, H. N. 1893. Extinct Monsters: A Popular Account of Some of the Larger Forms of Ancient Animal Life. Chapman and Hall, London, 362 p.

Hutchinson, J. R., K. T. Bates, J. Molnar, V. Allen, and P. J. Makovicky. 2011. A computational analysis of limb and body dimensions in *Tyrannosaurus rex* with implications for locomotion, ontogeny, and growth. PLoS ONE 6(10):1–20.

Ketchum, H. F., and R. B. J. Benson. 2010. Global interrelationships of Plesiosauria (Reptilia, Sauropterygia) and the pivotal role of taxon sampling in determining the outcome of phylogenetic analyses. Biological Reviews 85(2):361–392.

Knutsen, E. M., P. S. Druckenmiller, and J. H. Hurum. 2012. Two new species of long-necked plesiosaurians (Reptilia: Sauropterygia) from the Upper Jurassic (Middle Volgian) Agardhfjellet Formation of central Spitsbergen. Norwegian Journal of Geology 92:187–212.

Kogan, I., S. Pacholak, M. Licht, J. W. Schneider, C. Brucker, and S. Brandt. 2015. The invisible fish: hydrodynamic constraints for predator-prey interaction in fossil fish *Saurichthys* compared to recent actinopterygians. Biology Open 4(12):1715–1726.

Kubo, T., M. T. Mitschell, and D. M. Henderson. 2012. *Albertonectes vanderveldei*, a new elasmosaur (Reptilia, Sauropterygia) from the Upper Cretaceous of Alberta. Journal of Vertebrate Paleontology 32(3):557–572.

Lauder, G. V., and P. G. A. Madden. 2006. Learning from fish: kinematics and experimental hydrodynamics for roboticists. International Journal of Automation and Computing 4:325–335.

Lautenschlager, S. 2017. Digital reconstruction of soft-tissue structures in fossils. The

Paleontological Society Papers 22:101–117.

Liu, S., A. S. Smith, Y. Gu, J. Tan, C. K. Liu, and G. Turk. 2015. Computer simulations

imply forelimb-dominated underwater flight in plesiosaurs. PLoS Computational

Biology 11(12):e1004605.

Long, J. H., JR., J. Schumacher, N. Livingston, and M. Kemp. 2006. Four flippers or two?

Tetrapodal swimming with an aquatic robot. Bioinspiration and Biomimetics

1(1):20–29.

Maresh, J. L., F. E. Fish, D. P. Nowacek, S. M. Nowacek, and R. S. Wells. 2004. High

performance turning capabilities during foraging by bottlenose dolphins (*Tursiops

truncatus*). Marine mammal science 20(3):498-509.

Martin, J. E., E. Frey, and J. Riess. 1986. Soft tissue preservation in ichthyosaurs and a

stratigraphic review of the Lower Hettangian of Barrow-upon-Soar, Leicestershire.

Transactions of the Leicester Literary and Philosophical Society 80:58–72.

Massare, J. A. 1988. Swimming capabilities of Mesozoic marine reptiles: implications for

method of predation. Paleobiology 14(2):187–205.

Massare, J. A. 1994. Swimming capabilities of Mesozoic marine reptiles: a review, p. 133–

149, Mechanics and Physiology of Animal Swimming. Cambridge University Press,

Cambridge.

McGowan, C. 1999. A Practical Guide to Vertebrate Mechanics. Cambridge University

Press, 316 p.

McHenry, C. R., A. G. Cook, and S. Wroe. 2005. Bottom-feeding plesiosaurs. Science

310(5745):75.

McHenry, M. J., P. S. L. Anderson, S. Van Wassenbergh, D. G. Matthews, A. P. Summers, and S. N. Patek. 2016. The comparative hydrodynamics of rapid rotation by predatory appendages. Journal of Experimental Biology 219:3399–3411.

Motani, R. 2002. Swimming speed estimation of extinct marine reptiles: energetic approach revisited. Paleobiology 28(2):251–262.

Muscutt, L. E., G. J. Dyke, G. D. Weymouth, D. Naish, C. Palmer, and B. Ganapathisubramani. 2017. The four-flipper swimming method of plesiosaurs enabled efficient and effective locomotion. Proceedings of the Royal Society B 284(1861):1–8.

Nagesan, R. S., D. M. Henderson, and J. S. Anderson. 2018. A method for deducing neck mobility in plesiosaurs, using the exceptionally preserved *Nichollssaura borealis*. Royal Society Open Science 5(8): 172307.

Noè, L. F., M. A. Taylor, and M. Gómez-Pérez. 2017. An integrated approach to understanding the role of the long neck in plesiosaurs. Acta Palaeontologica Polonica 62(1):137–162.

O'Gorman, J. P., and M. S. Fernandez. 2016. Neuroanatomy of the vertebral column of *Vegasaurus molyi* (Elasmosauridae) with comments on the scervico-dorsal limit in plesiosaurs. Cretaceous Research 73:91–97.

O'Keefe, F. R. 2001. Ecomorphology of plesiosaur flipper geometry. Journal of Evolutionary Biology 14:987–991.

O'Keefe, F. R. 2002. The evolution of plesiosaur and pliosaur morphotypes in the Plesiosauria (Reptilia: Sauropterygia). Paleobiology 28(1):101–112.

O'Keefe, F. R., and M. T. Carrano. 2005. Correlated trends in the evolution of the plesiosaur locomotor system. Paleobiology 31(4):656–675.

O'Keefe, F. R., and N. Hiller. 2006. Morphologic and ontogenetic patterns in elasmosaur
neck length, with comments on the taxonomic utility of neck length variables.
Paludicola 5:206-229.

Otero, R. A. 2016. Taxonomic reassessment of *Hydralmosaurus* as *Styxosaurus*: new
insights on the elasmosaurid neck evolution throughout the Cretaceous. PeerJ
4:e1777.

Pierce, S. E., J. A. Clack, and J. R. Hutchinson. 2011. Comparative axial morphology in
pinnipeds and its correlation with aquatic locomotory behaviour. Journal of Anatomy
219(4):502-514.

Rahman, I. A. 2017. Computational fluid dynamics as a tool for testing functional and
ecological hypotheses in fossil taxa. Palaeontology 60(4):451–459.

Rahman, I. A., S. A. F. Darroch, R. A. Racicot, and M. Laflamme. 2015a. Suspension
feeding in the enigmatic Ediacaran organism *Tribrachidium* demonstrates complexity
of Neoproterozoic ecosystems. Science advances 1(10):1–9.

Rahman, I. A., and S. Lautenschlager. 2017. Applications of three-dimensional box
modeling to paleontological functional analysis. The Paleontological Society Papers
22:119–132.

Rahman, I. A., S. Zamora, P. L. Falkingham, and J. C. Phillips. 2015b. Cambrian cinctan
echinoderms shed light on feeding in the ancestral deuterostome. Proceedings of the
Royal Society B 282:1–7.

Rivera, G., A. R. V. Rivera, E. E. Dougherty, and R. W. Blob. 2006. Aquatic turning
performance of painted turtles (*Chrysemys picta*) and functional consequences of a
rigid body design. The Journal of Experimental Biology 209(21):4203-4213.

Rothschild, B. M. 1982. Rheumatology: A Primary Care Approach. Yorke Medical Press, New York, 416 p.

Rothschild, B. M. 1987. Decompression syndrome in fossil marine turtles. Annals of the Carnegie Museum 56:253–258.

Rothschild, B. M. 1991. Stratophenetic analysis of avascular necrosis in turtles: affirmation of the decompression syndrome hypothesis. Comparative Biochemistry and Physiology Part A: Physiology 100(3):529–535.

Rothschild, B. M., and L. D. Martin. 1987. Avascular necrosis: occurence in diving Cretaceous mosasaurs. Science 236:75–78.

Rothschild, B. M., and G. W. Storrs. 2003. Decompression syndrome in plesiosaurs (Sauropterygia: Reptilia). Journal of Vertebrate Paleontology 23(2):324–328.

Rudwick, M. J. S. 2008. Worlds before Adam: The reconstruction of Geohistory in the Age of Reform. University of Chicago Press, Chicago and London, 639 p.

Sachs, S., J. J. Hornung, and B. P. Kear. 2016. Reappraisal of Europe's most complete Early Cretaceous plesiosaurian: *Brancasaurus brancai* Wegner, 1914 from the "Wealden facies" of Germany. PeerJ 4:e2813.

Sachs, S., B. P. Kear, and M. J. Everhart. 2013. Revised vertebral count in the "longest-necked vertebrate" *Elasmosaurus platyurus* Cope 1868, and clarification of the cervical-dorsal transition in Plesiosauria. PLoS One 8(8):e70877.

Sato, T., Y. Hasegawa, and M. Manabe. 2006. A new elasmosaurid plesiosaur from the Upper Cretaceous of Fukushima, Japan. Palaeontology 49(3):467–484.

Segre, P. S., D. E. Cade, F. E. Fish, J. Potvin, A. N. Allen, J. Calambokidis, A. S. Friedlaender, and J. A. Goldbogen. 2016. Hydrodynamic properties of fin whale

flippers predict maximum rolling performance. Journal of Experimental Biology 219(21):3315–3320.

Serratos, D. J., P. S. Druckenmiller, and R. B. J. Benson. 2017. A new elasmosaurid (Sauropterygia, Plesiosauria) from the Bearpaw Shale (Late Cretaceous, Maastrichtian) of Montana demonstrates multiple evolutionary reductions of neck length within *Elasmosauridae*. Journal of Vertebrate Paleontology 37(2): e1278608.

Shuler, E. W. 1950. A new elasmosaur from the Eagle Ford Shale of Texas. Fondren Science Series 1(2):1–33.

Smith, A. S. 2007. Anatomy and systematics of the Rhomaleosauridae (Sauropterygia: Plesiosauria), University College Dublin, Dublin, 301 p.

Smith, A. S., and R. Araújo. 2017. *Taumatodracon wiedenrothi*, a morphometrically and stratigraphically intermediate new rhomaleosaurid plesiosaurian from the Lower Jurassic (Sinemurian) of Lyme Regis. Palaeontographica, Abt. A: Palaeozoology – Stratigraphy 308(4-6):89-125.

Smith, A. S., and P. Vincent. 2010. A new genus of pliosaur (Reptilia: Sauropterygia) from the Lower Jurassic of Holzmaden, Germany. Palaeontology 53(5):1049–1063.

Soul, L. C., and R. B. J. Benson. 2017. Developmental mechanisms of macroevolutionary change in the tetrapod axis: A case study of Sauropterygia. Evolution 71(5):1164–1177.

Stevens, L. M., R. W. Blob, and C. J. Mayerl. 2018. Ontogeny, morphology and performance: changes in swimming stability and turning performance in the freshwater pleurodire turtle, *Emydura subglobosa*. Biological Journal of the Linnean Society 125(4):718-729.

Sutton, M., I. Rahman, and R. Garwood. 2017. Virtual paleontology - an overview. Paleontological Society Papers 22:1–20.

Taylor, M. A. 1981. Plesiosaurs - rigging and ballasting. Nature 290:628–629.

Van Wassenbergh, S., N. Z. Potes, and D. Adriaens. 2015. Hydrodynamic drag constrains head enlargement for mouthbrooding in cichlids. Royal Society Interface 12(109):20150461.

Van Wassenbergh, S., K. Van Manen, T. A. Marcroft, M. E. Alfaro, and E. J. Stamhuis. 2014. Boxfish swimming paradox resolved: forces by the flow of water around the body promote manoeuvrability. Journal of The Royal Society Interface 12(103):20141146.

Vanburen, C. S., and D. C. Evans. 2016. Evolution and function of anterior cervical vertebral fusion in tetrapods. Biological Reviews 92(1):608–626.

Versteeg, H. K., and W. Malalasekera. 2007. An Introduction to Computational Fluid Dynamics - The Finite Volume Method. 2nd edition. Longman Scientific & Technical, Harlow, 267 p.

Vincent, P., R. Allemand, P. D. Taylor, G. Suan, and E. E. Maxwell. 2017. New insights on the systematics, palaeoecology and palaeobiology of a plesiosaurian with soft tissue preservation from the Toarcian of Holzmaden, Germany. Science of Nature 104(51):1–13.

Vogel, S. 1989. Life in moving fluids: The physical biology of flow. Princeton University Press, 352 p.

Vogel, S. 2013. Comparative biomechanics: life's physical world. 2nd edition. Princeton University Press, 640 p.

Walker, J. A. 2000. Does a rigid body limit maneuverability? Journal of Experimental Biology 203(22):3391-3396.

Watson, D. M. S. 1924. The elasmosaurid shoulder-girdle and fore-limb. Proceedings of the Zoological Society of London 94(3):885–917.

Weihs, D. 2002. Stability versus maneuverability in aquatic locomotion. Integrative and Comparative Biology 42(1):127-134.

Welles, S. P. 1943. Elasmosaurid plesiosaurs with description of new material from California and Colorado. Memoirs of the University of California 13:125–254.

Welles, S. P. 1952. A review of the North American Cretaceous elasmosaurs. University of California Publications in Geological Sciences 29:47–144.

Welles, S. P., and J. D. Bump. 1949. *Alzadasaurus pembertoni*, a new elasmosaur from the Upper Cretaceous of South Dakota. Journal of Vertebrate Paleontology 23(5):521–535.

Wilkinson, D. M., and G. D. Ruxton. 2012. Understanding selection for long necks in different taxa. Biological Reviews of the Cambridge Philosophical Society 87(3):616–630.

Wilson, D. E., and R. A. Mittermeier. 2014. Sea mammals. Handbook of Mammals of the World.Volume 4. Lynx Edicions, Barcelona, 614 p.

Wilson, R. P., A. Gómez-Laich, J.-E. Sala, G. Dell´Omo, M. D. Holton, and F. Quintana. 2017. Long necks enhance and constrain foraging capacity in aquatic vertebrates. Proceedings of the Royal Society B 284(1867):1–8.

Witmer, L. M. 1995. The extant phylogenetic bracket and the importance of reconstructing soft tissues in fossils; pp. 19-33 *in* J. J. Thomason (ed.), Functional Morphology in Vertebrate Paleontology. Cambrigde University Press, Cambridge.

Zammit, M., C. B. Daniels, and B. P. Kear. 2008. Elasmosaur (Reptilia: Sauropterygia) neck

    flexibility: implications for feeding strategies. Comparative Biochemistry and

    Physiology Part A: Molecular & Integrative Physiology 150(2):124–130.

Zarnik, B. 1925. K etologiji plesiosaurija, sa primosima mehanici kralježnice u recentnih

    sauropsida. Glasnik Nauč. Casopis Prirod. Društvo 38(39):424–479.
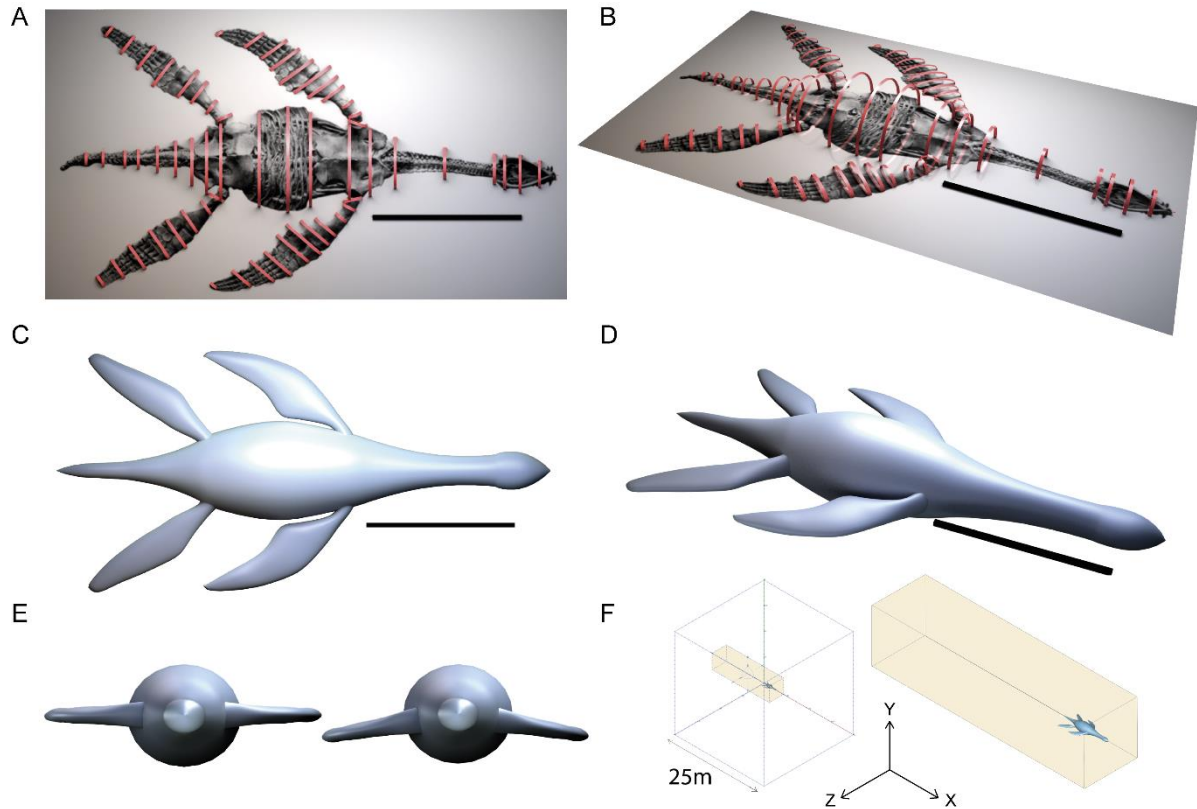
Final word count: 10973

FIGURE 1. Dorsal (**A**) and isometric (**B**) view of the plesiosaur model constructed using NURBs circles around photograph from Smith and Vincent (2010). Dorsal (**C**) and isometric (**D**) view of closed body cavities surfaces were then generated by 'lofting' a continuous surface through consecutive NURBS circles to produce discrete body volumes for each segment. Frontal view lofted plesiosaur model showing even flippers and at 10 degrees angle from centre of body (**E**). Full computational domain including X, Y, Z-directions of the 3D coordinate system and refined region (yellow) (**F**). [Intended for page width 182.033mm, height 123.406mm]
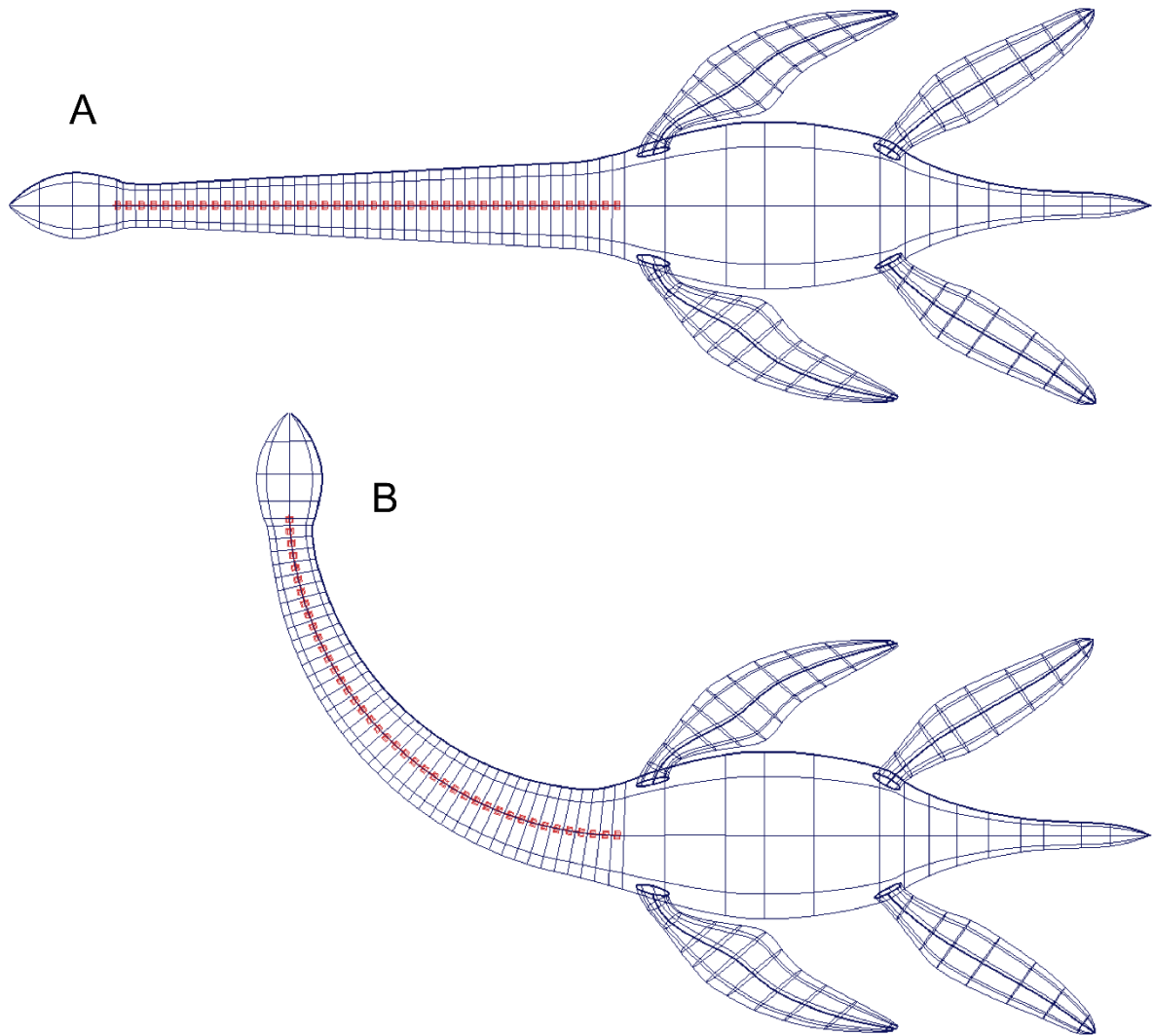
FIGURE 2. Example of the rigging for the idealized plesiosaur models. Dorsal view of the

skeleton for the plesiosaur model with intermediate neck including joints and cylinders in the

centre of the neck (coloured in red) inserted to illustrate each cervical vertebra. (**A**) Model

with straight neck and (**B**) model with the neck bent 90°. [Intended for page width

182.033mm, height 163.584mm]
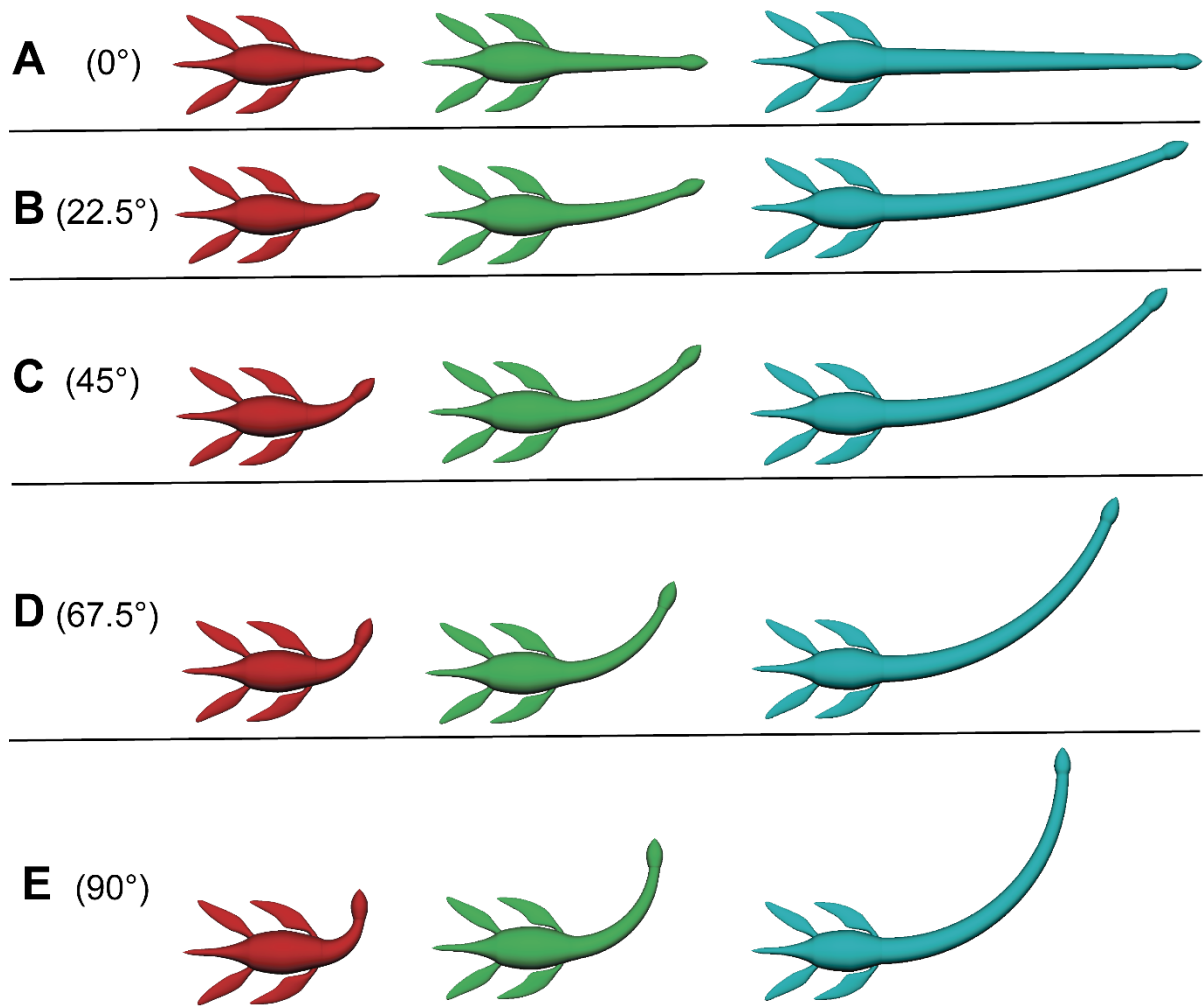
FIGURE 3. Illustration of the short-necked (red), intermediate (green), and long-necked (cyan) idealized plesiosaur models shown as straight (**A**) and with the four stages of total neck curvature of (**B**) 22.5°, (**C**) 45°, (**D**) 67.5° and (**E**) 90°. [Intended for page width 182.033mm, height 152.156mm]
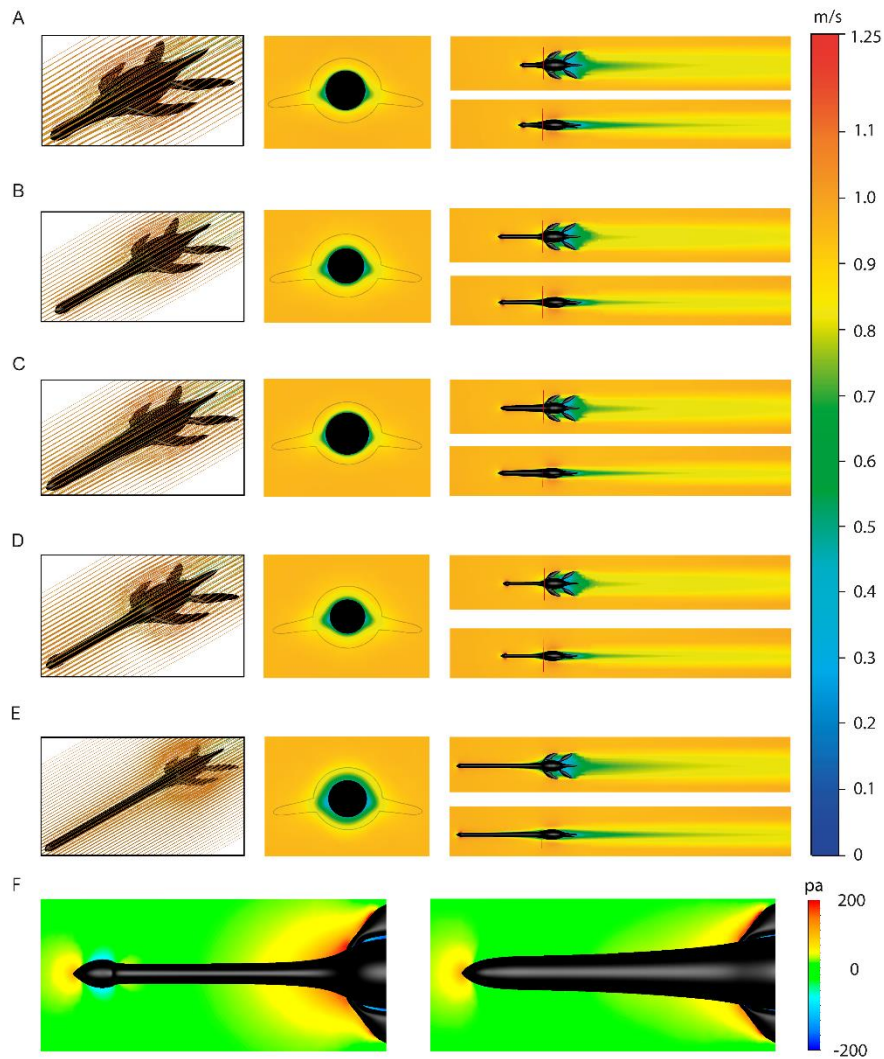
FIGURE 4. Three-dimensional flow velocity pattern surrounding plesiosaur models at 1m/s creating flows of different velocities in the wake shown with flow traces (left images) and flow velocity magnitudes in frontal view (middle images) and dorsal/side view (right images). (**A**) Short neck, (**B**) intermediate neck, (**C**) thick neck, (**D**) thin neck, and (**E**) long neck. (**F**) close up of pressure around head and neck region in dorsal view of the thin neck (left image) and thick neck (right image). The direction of flow (left and right images) is from left to right. Red line (right images) indicated plane position on the models for frontal view. [Intended for page width 182.033mm, height 220.293mm]
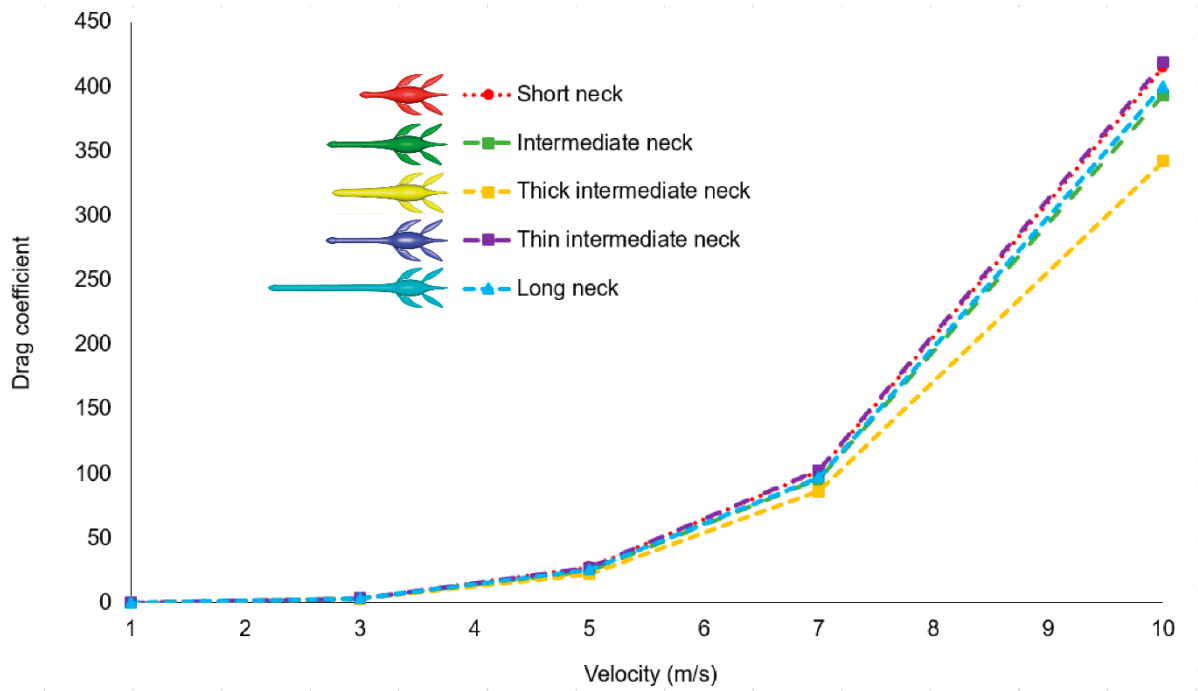
FIGURE 5. Simulation results using the five plesiosaur models with different neck lengths and thicknesses shown as velocity (m/s) against drag coefficient. Short neck (red), intermediate neck (green), thick neck using intermediate neck (yellow), thin neck using intermediate neck (purple), and long neck (blue). [Intended for page width 182.033mm, height 104.597mm]
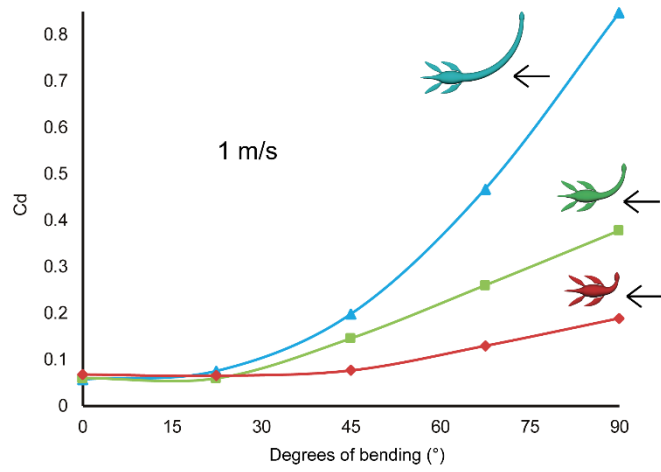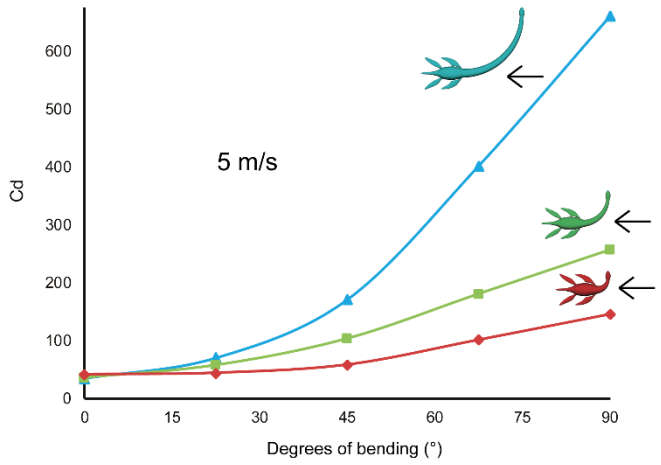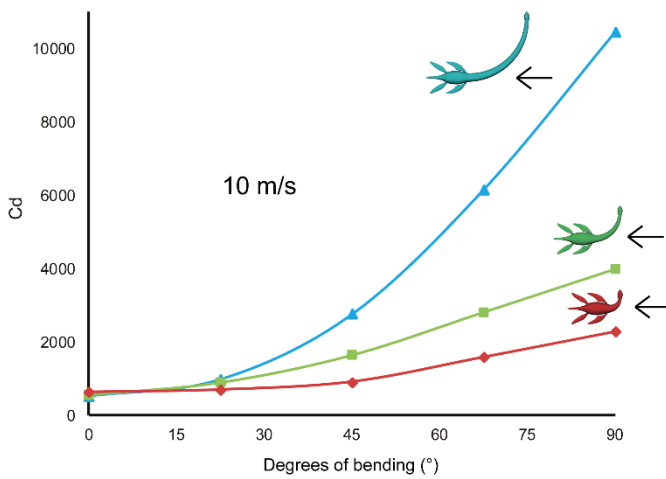
A

Cd (y-axis), Degrees of bending (°) (x-axis)

1 m/s

B

Cd (y-axis), Degrees of bending (°) (x-axis)

5 m/s

C

Cd (y-axis), Degrees of bending (°) (x-axis)

10 m/s

FIGURE 6. Frontal drag coefficients with increase in neck bending (0 – 90° with 22.5° interval) for the idealized plesiosaur models with short (red), intermediate (green), and long (blue) necks at (**A**) 1 m/s, (**B**) 5 m/s, and (**C**) 10 m/s. Drag force was calculated in negative X-direction of the 3D coordinate system indicated by arrows, using frontal area of the plesiosaur models to calculated drag coefficients. [Intended for column width 88.9mm, height 216.022mm]
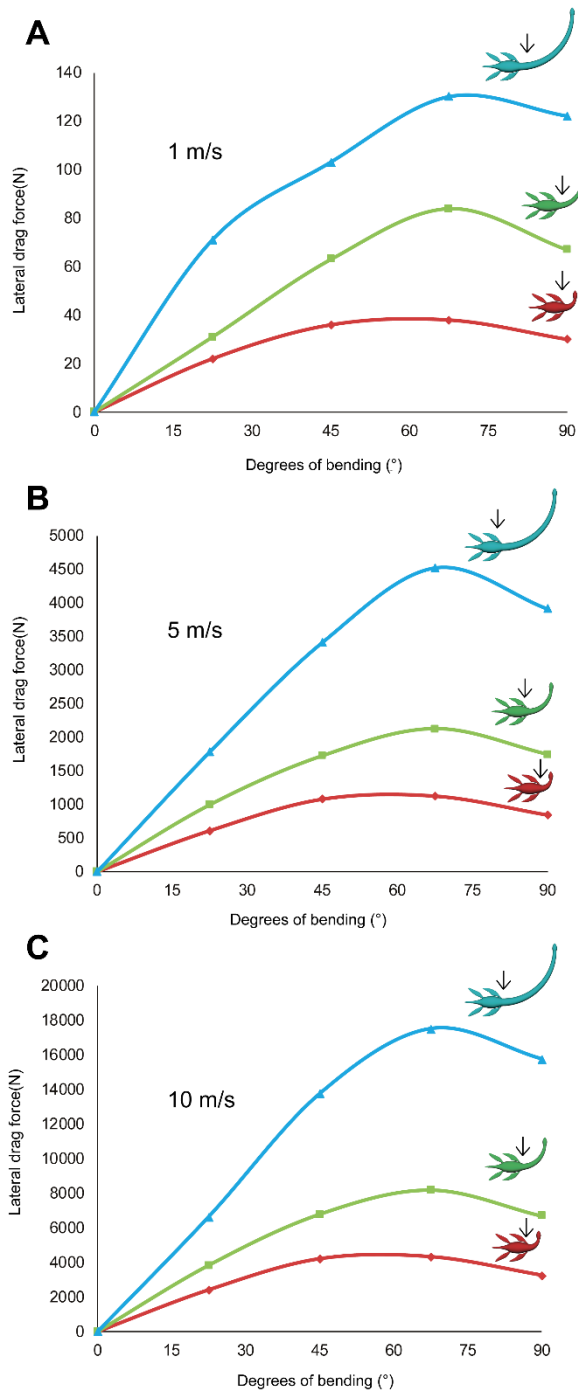
FIGURE 7. Lateral drag forces (N) with increase in neck bending (0 – 90° with 22.5° interval) for the idealized plesiosaur models with short (red), intermediate (green), and long (blue) necks at (**A**) 1 m/s, (**B**) 5 m/s, and (**C**) 10 m/s. Drag force was calculated in the negative Z-direction of the 3D coordinate system indicated by arrows. [Intended for column width 88.9mm, height 207.548mm]
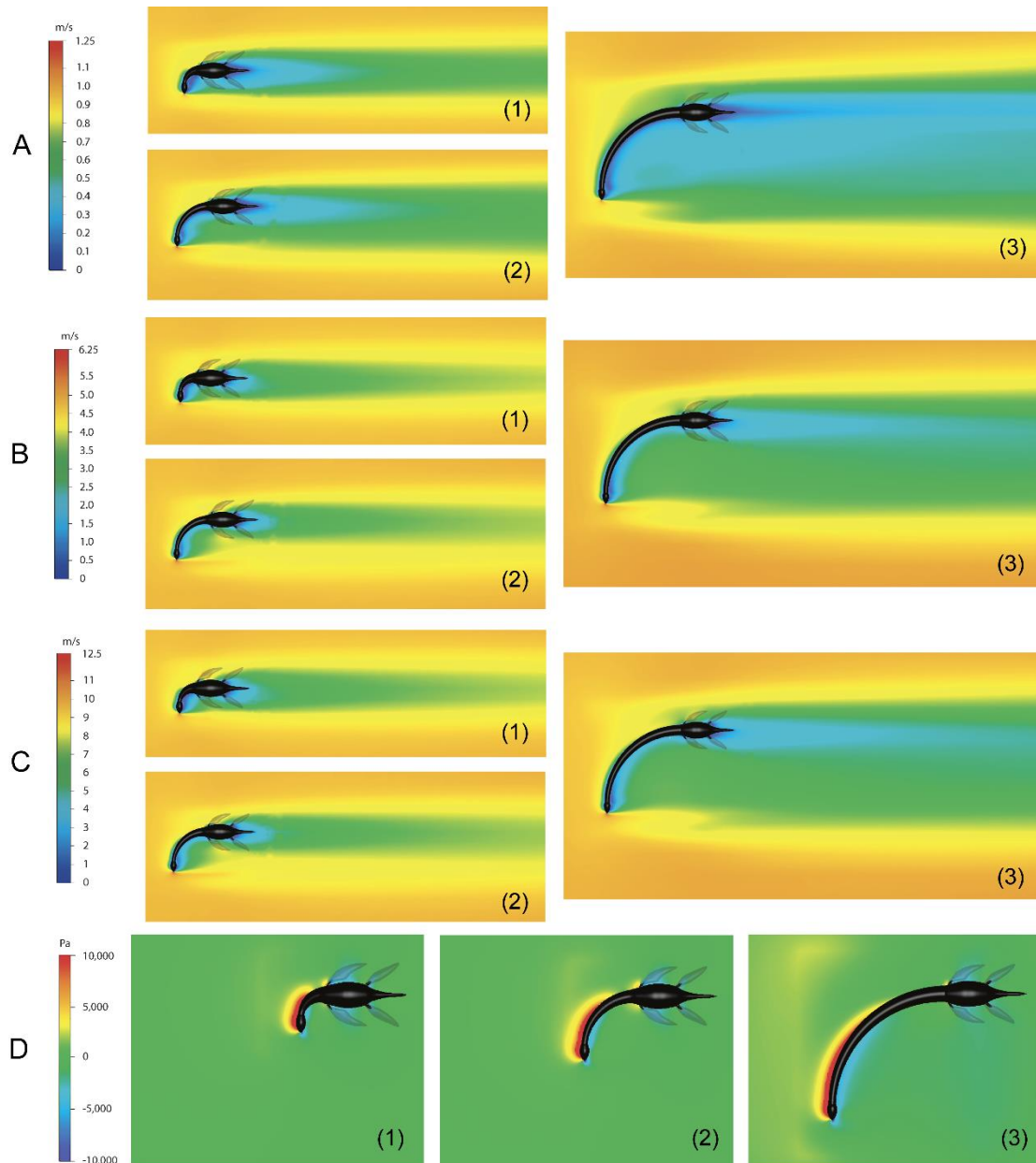
FIGURE 8. Flow velocity patterns (**A**-**C** and **E**) and pressure distributions (**D**) created by the water flow for the (**1**) short-, (**2**) intermediate, and (**3**) long-necked idealized plesiosaur models bended at 90°. (**A**) Top view of the flow velocity pattern at 1 m/s, (**B**) top view of the flow velocity pattern at 5 m/s, and (**C**) top view of the flow velocity pattern at 10 m/s. (**D**) Top view of pressure distribution at 5 m/s. Notice in **A**-**D** that the flippers were located below the planes cut midway through the body, as indicated by the transparent flippers. Flow inlet from left to right in **A**-**D**. [Intended for page width 182.033mm, height 203.642mm]
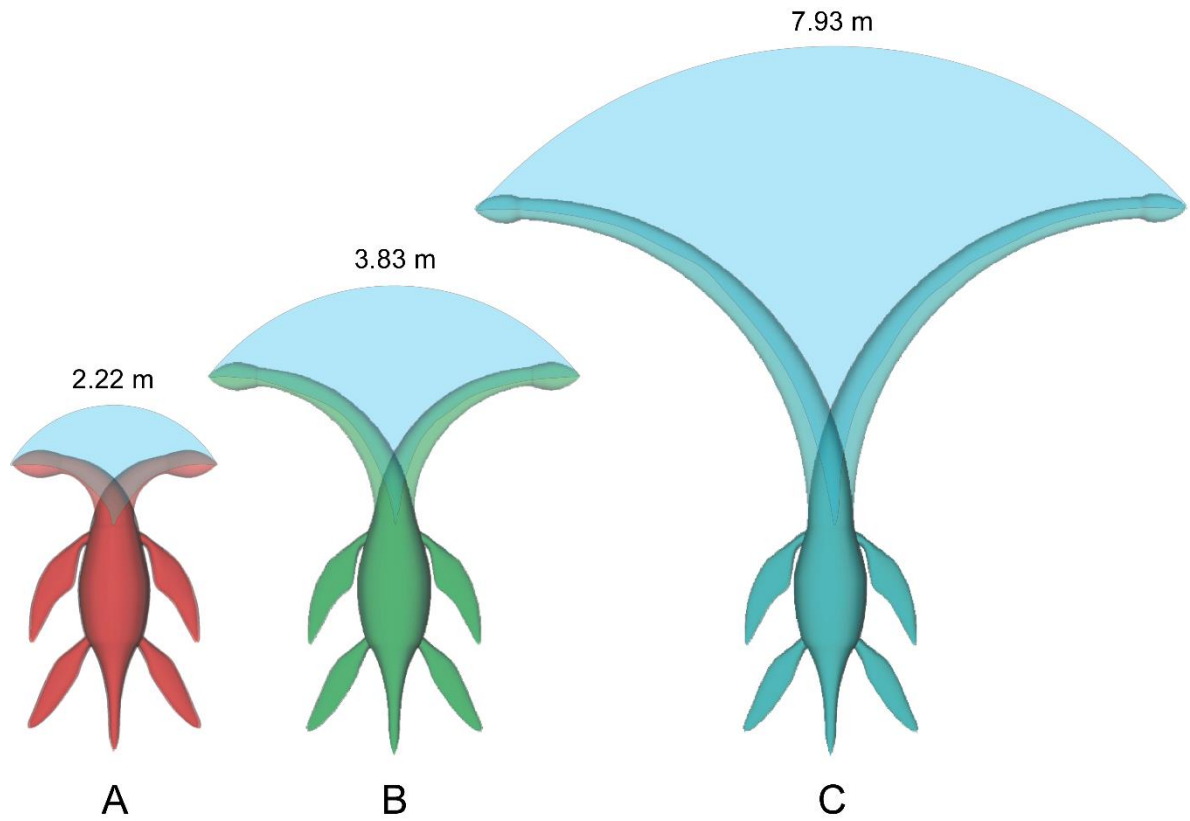
FIGURE 9. Potential feeding envelopes (blue circle slices) in lateral movements for the short-necked (**A**), intermediate-necked (**B**), and long-necked (**C**) plesiosaur models, including area (within circle slices), and arc length (on top of circles slices) for each plesiosaur model. [Intended for page width 182.033mm, height 124.769mm]